Author(s): Lahti, Riikka; Bergna, Davide; Romar, Henrik; Hu, Tao; Comazzi, Alberto; Pirola, Carlo; Bianchi, Claudia L.; Lassi, Ulla

Title: Characterization of Cobalt Catalysts on Biomass-Derived Carbon Supports

Year: 2017

Version:

Please cite the original version:

Lahti, R., Bergna, D., Romar, H., Hu, T., Comazzi, A., Pirola, C., Bianchi, C. L., & Lassi, U. (2017). Characterization of Cobalt Catalysts on Biomass-Derived Carbon Supports. Topics in Catalysis, 60(17-18), 1415-1428. https://doi.org/10.1007/s11244-017-0823-z

Characterization of cobalt catalysts on biomass-derived carbon supports

Riikka Lahti[1,2,*], Davide Bergna[1,2], Henrik Romar[1,2], Tao Hu[1],

Alberto Comazzi[3], Carlo Pirola[3], Claudia L. Bianchi[3], Ulla Lassi[1,2]

[1] University of Oulu, Research Unit of Sustainable Chemistry, P.O.Box 3000, FI-90014 University of Oulu, Finland

[2] University of Jyvaskyla, Kokkola University Consortium Chydenius, Applied Chemistry, P.O.Box 567, FI- 67101 Kokkola, Finland

[3] Università degli Studi di Milano, Dipartimento di Chimica, Via Golgi, 19 - 20133 Milano, Italy

** E-mail address:* riikka.lahti@chydenius.fi

Abstract

Cobalt catalysts are known to have a high activity and selectivity in the Fischer-Tropsch reaction converting synthesis gas to higher hydrocarbons (C_{5+}). These catalysts have been supported by different porous materials. Porous carbon materials like activated carbon (AC) have physical and chemical surface properties that affect the preparation of supported metal catalysts and can easily be tailored.

In this study, AC was produced by carbonization and steam activation of lignin, a waste fraction from the Kraft pulping process. A series of Co/AC-catalysts was produced and characterized by several techniques. According to the results, tailored properties (high surface area, mesoporosity) were obtained for carbon supports. Further, ash content could be reduced by acid treatment. Co/AC-catalysts prepared by ultrasonic assisted impregnation have high metal dispersion (10.1%). It was also observed that small metal particles were difficult to reduce, but acid (HNO_3) treatment has a positive effect on reduction temperatures.

Keywords: activated carbon, catalyst, characterization, cobalt**,** support

1. Introduction

The sustainable catalytic conversion of renewable resources to chemicals and fuels is a rapidly growing field in research. Practically all fuels and over 85% of the chemicals coming out of petrochemical refineries have seen at least one catalytic conversion step in their production process. Conventional catalysts have been supported by a number of supports, such as Al_2O_3, SiO_2, and TiO_2. Many recent reviews deal with the advantages of carbon supports for the preparation of highly dispersed metal catalysts. Porous carbon materials like activated carbon (AC) have physical and chemical surface properties that can easily be such as a large surface area, the proper pore size distribution and acid-base characters on the surface that affect to the preparation of metal supported catalysts.[1-3]

Cobalt-based catalysts are known to have a high activity in the Fischer-Tropsch reaction (FT) converting synthesis gas into linear hydrocarbons and waxes and have low activity for the water gas shift reaction. Many studies have been done with different preparation methods, cobalt loading, and supports.[4-9] It has been found that the support materials have a significant role on the activity of the heterogeneous catalysts. However, a strong metal-support interaction between cobalt and conventional oxide supports (Al_2O_3, SiO_2, etc.) inhibits the formation of catalytically active high dispersed metal.[10,11] It is known that obtain optimal catalytic FT performance both high surface area and a well-developed porosity are very important for achieving a high dispersion of the active phase in the catalyst. Carbon materials, especially AC, has surface areas significantly higher than another conventional oxide catalyst supports increasing surface area and porosity of the carbon facilitates the loading of metal [12]. As a chemically inert material, carbon support can reduce the interaction with the cobalt species and increase the cobalt reducibility [13]. Advantageously carbon materials can be prepared from residual biomass and waste materials which is an attractive property for decreasing the so-called “carbon footprint” of a biomass transformation process [2]. Beside the high surface area carbon support also has many other advantages in the catalytic applications like tailored pore size distribution that can be modified for specific reactions, resistance to acidic or basic media, amphoteric character due to the presence of various oxygenated functional groups which enhances metal adsorption and catalyst dispersion, the structure that is stable at high temperatures, even above 700 °C (except in the

presence of oxygen >200 °C and for hydrogenation reactions >400 °C), less expensive compared to alumina and silica supports; porous carbons can be prepared in different physical forms (granules, extrudates, pellets, fibers, cloths, etc.), hydrophobic carbon can be modified to increase the hydrophilicity and active phase can be recovered by eliminating the support through burning away the carbon. [2]

By modifying the carbon support, surface pore structure and functional groups (O, N, H) supported Co-catalysts with a high degree of reduction and high Co dispersion can be obtained. These functional groups are considered anchoring sites for cobalt particles on the surface of AC, which can increase the cobalt metal-loading, dispersion, and stability.[13] It has been observed that the more acidic the groups are, the less hydrophobic is the carbon surface, making the surface more accessible to the aqueous solution of the metal precursor upon impregnation. The metallic dispersion is said to increase with the increased amount of oxygen on the surface. Oxygen groups on the surface have been most studied since they are formed spontaneously by exposure of the material to the atmosphere during the activation process. The concentration of these groups can be increased with different oxygenation treatments such as nitric acid disposal. Fixation of the acidic groups on the surface of the AC makes the surface more hydrophilic, decreases its pH, and increases the negative surface charge density. These treatments can also affect the surface area and pore texture of the activated carbons. [12, 14, 15]

Mesopore volume and mean mesopore size have been reported to be important parameters to control metal particle size and dispersion on carbon materials. A support with modified mesoporous and macroporous structure can have excellent advantages in FT reaction because larger pores benefits rapid molecular transportation and enhances the production for longer hydrocarbon chain distribution. The microporous structure of activated carbon is claimed to result in high methane and light hydrocarbon selectivity. [13,16]

A number of studies have been shown that addition of noble metals has a strong impact on the activity and selectivity on cobalt catalysts. The addition of noble metal promoters can shift the temperature needed to reduce cobalt oxide to metallic cobalt to lower temperatures, but its effect on the degree of reduction has been reported to be rather minor. Instead, the improved activity of noble metal promoted cobalt catalysts has been mainly attributed to higher cobalt dispersions. [17-19]

Many activated carbons have reported having high ash content. Ash content has a relatively small, but significant negative effect on the adsorption of the metal precursor. By selecting an appropriate precursor and modifying the carbon with different treatments, it is possible to prepare porous carbons with very low ash content. [2, 3]

Preparation of carbon supported metal catalyst can be done with impregnation methods, precipitation methods or by ion-exchange method. With impregnation methods, incipient wetness method is performed in which the metal precursor is dissolved in small amount of solvent just enough to fill the pores of the support. Cobalt-based catalysts are relatively seldom prepared with precipitation methods but few papers have been published. [20-24]

In this study, a series of unpromoted and promoted cobalt catalysts supported on AC used as such or modified by different acid treatments have been prepared and characterized. Effect of acid pretreatments (HCl and HNO_3) on AC and different preparation methods including impregnation methods and precipitation methods have been studied. Also, the effect of promoting the cobalt catalysts with noble metals ruthenium and rhenium have been tested in this study.

2. Experimental

2.1 Preparation of activated carbon

The lignin was dried and sieved to obtain particles of 0.8-1.2 mm in diameter. The sieved lignin was carbonized and steam activated in a one-step process in a rotating quartz reactor (Nabertherm GmbH RSRB 80). The thermal profile during the whole process was divided into two parts: the first carbonization step, in which the temperature was raised to 800 °C with a ramp of 6.7 °C /min, procured the total carbonization of the lignin followed by the activation step. During the activation temperature was kept at 800 °C for 120 min with a stream of water steam (120 g/h at 140 °C), created the proper surface activation. During the whole process, the reactor was flushed with an inert gas, in ramping step only N_2 (flow 200 ml/min) and in activation step carrier gas (N_2 flow 200 ml/min) and steam (120 g/h at 140 °C). The resulting AC was characterized for ash content, carbon content (TC), specific surface area, and pore size distribution.

2.2 Preparation of catalysts

The formed AC was crushed and fractioned by sieving into particle size 50-100 µm. Some of the carbon was used as such, other parts either acid-treated with hydrochloric acid (HCl) in order to demineralize the sample or oxidized with nitric acid (HNO_3) in order to introduce functional groups into the carbon. Acid treatments were performed with 30 wt. % HCl or with 10 wt. % HNO_3 refluxed 3h and washed with distilled H_2O until pH was neutral. Finally, the AC was dried overnight at 105 °C. AC demineralized with HCl was used as a support in the preparation of catalyst AC-HCl-Co-IW and AC oxidized with HNO_3 was used as a support in the preparation of catalysts AC-HNO_3-Co-IW. AC-Co-IW was prepared by incipient wetness impregnation of cobalt as such without any pretreatment of AC. Cobalt catalysts containing 10 wt. % of Co were prepared by incipient wetness impregnation of the ACs using $Co(NO_3)_3$*6 H_2O as a precursor. Promoter metals ruthenium or rhenium were added in some catalysts using precursor metal salts $Ru(NO)(NO_3)_3$ (AC-CoRu-IW) or ReO_4H (AC-CoRe-IW) in order to get 0.2 wt. % promoter metal on the catalyst. Promoter metal was added to precursor solution and performed one-step incipient wetness impregnation. After impregnation, the catalysts were dried overnight at 105 °C and calcined at 320 °C for 16 hours. The calcination step was performed in a quartz reactor placed into a tubular oven and flushed with nitrogen (240 ml/h/g_{cat}) during the whole process. Beside incipient wetness impregnation method, precipitation method was used in the preparation of AC-Co-PR catalyst. The cobalt precursor $Co(NO_3)_3$*6 H_20 was dissolved in distilled H_2O together with urea in a molar ratio of cobalt to urea of 1:2, and AC. The resulting solution was heated to 80 °C and stirred overnight to precipitate the cobalt. Finally, the impregnated AC was dried overnight at 105 °C before calcination. With catalyst AC-Co-US, ultrasonic assisted impregnation method was performed using an ultrasonic bath (VWR USC 200 TH, 45 kHz) during the addition of precursor solution ($Co(NO_3)_3$*6 H_20 dissolved in water) with a total US exposure time equal to 60 min at room temperature. After sonication, catalyst was rotated overnight in a rotating mixer (Rotavapor) and then dried overnight at 105 °C. The calcination step was performed in the same way for all catalysts as described above. A summary of the catalysts prepared and the preparation methods of Co/AC-catalysts are presented in Table 1 and Figure 1.

2.3 Catalyst characterization

The resulting catalysts (see Table 1) were characterized by a number of methods including elemental analysis, nitrogen physisorption, ICP-OES, SEM, TEM, DRIFT, XPS, XRD, and TPR analysis.

2.3.1 Total carbon and ash contents

The percentage of total carbon present in prepared ACs was measured using Skalar Primacs MCS instrument. Dried samples were weighted in quartz crucibles, combusted at 1100 °C in a pure oxygen atmosphere and the formed CO_2 was analyzed by an IR analyzer. The total mass of carbon in each sample was calculated as a percent of the mass initially weighted.

All samples were analyzed for ash content. A known amount of AC was transferred to tared crucibles and combusted in a muffle furnace for two hours at 815 °C with an initial temperature ramp of 9 °C /min. The ash contents were calculated as a percent of the initial dried biomass.

2.3.2 Surface areas and pore distribution

Specific surface areas and pore size distributions were calculated from adsorption isotherms of N_2 at isothermal conditions in liquid nitrogen according to the BET (Brunauer–Emmett–Teller) theory. Pore distribution was calculated from the adsorption isotherms using the BJH (Barrett–Joyner–Halenda) method. Each sample (about 100mg) was weight in a quartz tube. Samples were evacuated and heated in order to remove any adsorbed components and moisture. Evacuated samples were measured under isothermal conditions by Micromeritics ASAP 2020.

2.3.3 Metal content, dispersions and particle sizes

Metal contents of samples were measured by inductively coupled optical emission spectrometry (ICP-OES) using a Perkin Elmer Optima 5300 DV ICP–OES instrument. 0.10-0.12 g samples were added in 37 %

hydrochloric acid and 63 % nitric acid, then digesting in a microwave oven (MARS, CEM Corporation) at 200 °C for 10 min. After digestion, the solution was diluted to 50 ml and measured by ICP-OES.

Metal dispersions and particle sizes were measured from calcined samples by chemisorption of carbon monoxide (CO) assuming that stoichiometric ratio of was 1:1 between the adsorbent and cobalt (CO: Co) [25-26]. Each sample (about 500 mg) was weight in a U-shaped quartz tube and the sample was supported with glass wool. Prior to measurements, the sample was evacuated followed by a reduction in a stream of hydrogen (H_2) at 350 °C. Measurements were done using a Micromeritics ASAP 2020.

2.3.4 Catalyst morphology

A field emission scanning electron microscope (FESEM) Zeiss Ultra Plus equipped with and energy-dispersive X-ray spectroscopy (EDS) analysis system at the Center of Microscopy and Nanotechnology, University of Oulu was used to study the microstructure of the catalysts and for elemental analyses.

The morphology of the catalyst particles dispersed in the microemulsion was studied using an energy filtered transmission electron microscope EFTEM (LEO 912 OMEGA EFTEM). The catalysts samples were dispersed in acetone and pretreated in an ultrasonic bath for several minutes. A small drop of the microemulsion was deposited on a copper grid pre-coated with carbon and then evaporated in air at room temperature. The particle size of the samples was measured from TEM images of each sample and given in a reasonable range. The accelerating voltage and emission current in the measurements were 120 kV and 8-15 µA, respectively, while the resolution of the instrument was 0.37 nm.

X-ray diffraction (XRD) patterns were recorded by a PANalytical X´Pert Pro X-ray diffraction equipment using monochromatic CuKα1 radiation (λ=1.5406 Å) at 45 kV and 40 mA. Diffractograms were collected in the 2θ range 5-80° at 0.017° intervals and with scan step time of 110 s. The crystalline phases and structures were analyzed by HighScore Plus.

2.3.5 Temperature programmed reduction and oxidation

The conventional temperature programmed reduction experiments (TPR) were performed using a Thermoquest Mod. TPR/D/O 1100 (TCD detector) by feeding 30 ml/min of a 5.1% v/v H_2 in Ar gas mixture while heating by 8 °C/min from 50 °C up to 900 °C. The samples have been initially pre-treated in a flow of argon at T= 200 °C for 0.5 h. The TPR profiles of the catalysts exhibit hydrogen consumption peaks attributed to two-step reduction of Co_3O_4 to metallic cobalt with intermediate phase consisting mainly of CoO but most likely other hard-reduced cobalt oxides are present in the second peak.

(1) $Co_3O_4 + H_2 \rightarrow 3\ CoO + H_2O$

(2) $3\ CoO + 3\ H_2 \rightarrow 3\ Co^0 + 3\ H_2O$

The degree of reduction for the catalysts was measured on a Micromeritics Autochem by reoxidation of reduced catalysts. Small portions, about 25 mg, of each catalyst were weighed into a quartz tube. Prior to analysis, the samples were dried at 100 °C for 1 hour and then reduced for 1 hour at 350 °C in a flow of 10 % H_2 in Ar according to reactions (1) and (2). Co surface was rinsed with He flow until the signal from the TCD detector returned to the baseline. Small pulses of oxygen (5 % in He) were added using a calibrated loop until signals with a constant area were obtained. Between the pulses, the signal was allowed to return to baseline before applying next pulse. The degree of reduction was calculated from the moles of oxygen consumed assuming that all Co^0 was oxidized to Co_3O_4 according to reaction (3) compared to the amount of oxygen theoretically needed for a complete re-oxidation of Co^0. Any oxidation of the promoter metals or other reductions/ oxidations of other Co-species were not considered in the calculations.

(3) $3\ Co^0 + 2\ O_2 \rightarrow Co_3O_4$

2.3.6 X-ray photoelectron spectroscopy

X-ray photoelectron spectroscopy (XPS) analysis was performed using a Thermo Fisher Scientific ESCALAB 250Xi XPS System at the Center of Microscopy and Nanotechnology, University of Oulu (Finland). The catalyst samples were placed on an Indium film. With pass energy of 20 eV, the spot size of 900 µm, the accuracy of the reported binding energy was ±0.2 eV. The Al, O, Co, Re or Ru, C, In and N were measured for all samples.

The measurement data were analyzed by Avantage V5. The monochromatic AlKα radiation (1486.7 eV) operated at 20 mA and 15 kV. Charge compensation was used to determine the presented spectra and the calibration of the binding energies (BE) were performed by applying the C1s line at 284.8 eV as a reference.

2.3.7 The Diffuse Reflectance Infrared Fourier Transform

The Diffuse Reflectance Infrared Fourier Transform (DRIFT) analyses were performed by Brüker PMA 50 Vertex 80v equipment. In the DRIFT measurements the sample was maintained in a nitrogen flow at 105 °C for 60 min for the removal of water, then the chamber was cooled down to 25 °C in a nitrogen atmosphere, Analyses resolution was 4 cm^{-1} and 100 scans/min. Activated carbon samples were mixed with KBr (1:300) in a mortar to obtain a homogenous powder.

3. Results and discussion

3.1 Characterization results

Characterization results of untreated and treated samples are presented in Table 2. The table presents surface areas, pore sizes, pore volumes, and distributions. Also, total carbon content and ash contents are presented in Table 2. According to these analyses, carbonization and steam activation increased the carbon content of the Kraft lignin remarkable. Surface area (see Table 2) increased from 4.6 to 810 m^2/g and carbon content from 65 to 96 %. According to ash content, treatment with acid removed ash/minerals from the AC. Treatment with HCl seemed to remove some ash (from 6.1 to 4.8 %) and treatment with HNO_3 removed all remaining (from 6.1 to 0.0 %) ash from the AC. HNO_3 treatment seemed to collapse some of the carbon structure observed from decreasing surface area, pore volume, and total carbon content. Instead, HCl treatment seemed to open some of the carbon pore structure that could be seen from the slight increase in BET surface area.

The surface area of AC produced from Kraft lignin was rather high, 810 m^2/g, (see Table 2) compared to conventionally used supports which surface area is approximately 200 m^2/g or less [27-29]. Pore distribution

231 according to BJH model of AC (see Table 2) was 32 % of micropores (diameter smaller than 2 nm), 62 % of
232 mesopores (diameter from 2 nm to 50 nm) and 6 % of macropores (diameter larger than 50 nm).

233 Elemental analysis (C, H, O, N) was performed for activated carbon samples before Co addition and a
234 summary of these results is presented in Table 3. Results from the elemental analysis showed that treatments
235 with acid HNO_3 and HCl increased the amount of hydrogen in the carbon support. Treatment with HNO_3
236 increased nitrogen content in the AC support but the amount of oxygen decreased to zero. According to the
237 literature, treatment with HNO_3 will increase oxygen at the carbon surface. In the results obtained from the
238 elementary analyses, no such increase could be measured.

239 Surface area, pore volume, pore size, cobalt metal dispersion, metal particle size and metal surface area of
240 prepared and calcined Co/AC-catalysts are presented in Table 4. Impregnation with metal precursor
241 decreased the BET surface area about 10-26 % within range AC-HNO_3-Co-IW< AC-Co-IW< AC-Co-PR< AC-
242 CoRe-IW< AC-CoRu-IW< AC-HCl-Co-IW< AC-Co-US. Pore volumes decreased about 10-32 % within range AC-
243 HNO_3-Co-IW< AC-Co-IW< AC-Co-PR< AC-CoRu-IW <AC-CoRe-IW< AC-HCl-Co-IW< AC-Co-US. With catalyst AC-
244 Co-US and AC-HCl-Co-IW, the BET surface areas and pore volumes decreased most (BET surface areas 26 %
245 and pore volumes 32-27 %). Since the decrease of the surface areas and pore volumes were in some cases
246 quite high it seems an indication to that there might be some other compounds involved for example nitrates
247 from the precursor. Also, there is a possibility that some treatments e.g. US might collapse some of the AC
248 surface structure.

249 According to CO-chemisorption results dispersion of cobalt ranged from 0.7-10.1 % (see Table 4) within range
250 AC-HCl-Co-IW< AC-CoRu-IW< AC-HNO_3-Co-IW< AC-CoRe-IW< AC-Co-IW< AC-Co-US. Compared to previous
251 studies [29] with conventional supported (Al_2O_3, SiC, TiO_2) cobalt dispersion in Co/AC-catalysts was quite
252 competitive and in some cases rather high, especially with catalyst AC-Co-US dispersion of Co was even high
253 as 10.1 %. Also, catalyst AC-Co-IW gave quite high values for the dispersion of cobalt metal, 8.6 %. Otherwise,
254 it was expected, and as it was discussed in introduction part that oxidation treatment leads to a higher
255 dispersion; treatment with HNO_3 did not lead any particularly high cobalt dispersion on the surface and the

metal dispersion of catalyst AC-HNO_3-Co-IW was 3.4 %. The reason for this might be that treatment with HNO_3 did not increase the oxygen content of the AC. Instead, treatment with HCl increased oxygen content in the AC (see Table 3) but also in this case no higher metal dispersion was observed, in fact, HCl treated AC proved to have the lowest dispersion from prepared Co/AC-catalysts. According to CO-chemisorption results addition of promoter metals did not give any particularly high metal dispersion and Ru- and Re-promoted catalysts were measured to have a metal dispersions of 3.2 % (AC-CoRu-IW) and 5.8 % (AC-CoRe-IW) respectively.

Metal contents of the catalysts were measured by ICP analysis. The expected concentration of cobalt added was 10 wt. % and concentration of ruthenium and rhenium were 0.2 wt. %. The measured concentrations of metals are presented in Table 5. Cobalt concentrations in catalysts were at the expected level around 10 wt. % except in catalyst AC-Co-IW which contained only 5.9 wt. % of cobalt. The reason for this might be the preparation step and miscalculation the amount of cobalt. The concentration of promoter metals was expected to be 0.2 wt. %. The concentration of promoter Ru was in desired concentration, 0.24 wt. %. Measured value of Re was 0.39 wt. %. This double sized value must have caused the preparation step in which the addition of a very small amount of liquid promoter was difficult. Other metals including calcium, iron, potassium, sodium and magnesium were also measured to verify if some traces of metal were left from the preparation process of AC. Acid treated catalysts AC-HCl-Co-IW and AC-HNO_3-Co-IW contained these metals less than 0.02%. The concentration of metal Ca was 0.02 wt. % and concentration of metals Fe, Na, K and Mg were 0.01 wt. % or less and could be expected that no interference from these metals should be present in catalytic use. Other catalysts (AC-Co-IW, AC-CoRu-IW, AC-CoRe-IW, and AC-Co-US) contained Ca <0.04 wt. %, Fe <0.06 wt. % and Mg <0.03 wt. % and these values were quite low. Instead, concentrations of Na and K were higher; Na <0.35 wt. % and K <0.11 wt. %. These metals might be traces from pulping process and might interfere the catalytic activity in a negative way. [30, 31]

SEM and TEM analyses were used to verify catalyst morphology. From FESEM and TEM images (Figure 2) taken from the catalyst AC-Co-IW can be observed that Co-particles size were around 10-20 nm which was

quite close to results from CO-chemisorption in which average Co particle size was determined to be 11.6 nm (Table 4). TEM images of AC-Co-IW also highlighted that the active metal was present in the form of spherical particles with dimensions of about 10-20 nm quite well distributed on the support surface.

SEM-EDS analyses were performed for calcined Co/AC-catalysts. The point analyze were performed at different locations and marked in the SEM images. All elements were auto-detected using Oxford Instruments INCA software. Figure 3 showed the SEM-EDS analyze sites for catalyst AC-HNO_3-Co-IW. From SEM-EDS analyses, only major components (C, O and Co) are shown in Table 6. The SEM-EDS analyses also indicated the addition of Co on the catalyst surface.

XRD measurements were performed for calcined but not reduced Co/AC-catalysts. XRD was used to confirm the presence of cobalt in the catalysts and also to verify metal particle size. From XRD diffraction patterns, it was observed that catalysts showed very broad peaks for Co oxides, indicating a high cobalt metal dispersion and/or amorphous phase of support [32,33]. Since the broad peaks detected from XRD patterns calculation of cobalt metal particle size, based on Scherrer equation was not reliable. However from the XRD diffraction pattern (Figure 4) broad peaks indicated to CoO (111) at 2theta=36.7° and CoO (200) at 2theta=42.6°, according to standard JCPDS file number (CoO 04-005-4912) which proved the presence of cobalt in catalysts.

3.2 Reducibility of catalysts

3.2.1 Temperature programmed reduction (TPR)

According to the literature [34] from the H_2-TRP profile of Co/AC-catalysts three major peaks could be found; the first peak at around 320 °C corresponding the reduction of Co_3O_4 to CoO and second high-temperature peak at 450 °C related to the reduction of CoO to metallic cobalt, the third broad peak maximum around 600 °C is attributed to methane formation which is originated from the reduction of surface functional groups on the AC surface by H_2. From the H_2-TRP profile (Figure 5) in some cases, a small peak at 100 °C was detected which is due to desorption of residue moisture adsorbed on the catalysts surface. Also, the weak reduction

peak at around 220 °C could be found and is due to decomposition of residual cobalt nitrate. The first reduction peak for all catalysts is found at temperature 320-380 °C and the intensity is about the same for all. With second peak reduction step corresponding to the reduction of CoO and cobalt oxides to Co^0 there is more variety with reduction temperatures from 370 to 490 °C. A summary of H_2-TPR reduction temperature shifts is presented in Table 7. The treatment with HNO_3 (AC-HNO_3-Co-IW) seemed to shift the second reduction step to a lower temperature at 370 °C

The influence of support material and interaction between support and metal oxide can be observed when AC supported catalysts was compared to the conventional SiO_2 supported catalyst synthesized and characterized in a previous work [35]. Carbon supported catalysts presented little higher reduction temperatures referred to the first reduction step with respect with traditional FT catalysts [36, 37]. The first peak of reduction Co_3O_4 to CoO was around 260 °C for silica supported (SiO_2-Co) and 320-380 °C for AC supported Co-catalysts while second peak related to the reduction of CoO to metallic cobalt showed remarkable lower temperature for AC supported catalysts compared to silica supported catalyst (SiO_2-Co), in fact, the average temperature of carbon supported catalyst is around T= 420 °C, while the reduction temperature for the transition from CoO to Co presented by the SiO_2 supported catalysts is equal to T= 780 °C due to the presence of Co-silicates species, which are hard reducible species [38].

3.2.2 Temperature programmed oxidation (TPO)

The degree of reduction (Table 8) was calculated from the theoretical value of moles of oxygen per consumed moles of oxygen using the measured Co metal content value from the ICP analysis (see Table 5). The addition of Re seemed to affect the reduction degree of the catalyst AC-CoRe-IW with the highest degree of reduction 72 %. Catalyst AC-HNO_3-Co-IW oxidized with HNO_3 had a degree of reduction 66 %. With catalyst AC-CoRe-IW, the degree of reduction was higher when compared to conventional CoRe-catalyst supported on Al_2O_3 from literature [39]. The lowest degree of reduction was calculated on catalysts AC-Co-US and it was equal to 25 %. Low values of reduction were measured also with catalysts AC-CoRu-IW (38 %) and AC-Co-IW (39

330 %). One of the reasons for the low degree of reduction might be explained due to rather small cobalt particle
331 sizes, which are harder to reduce. Overall, these values were well comparable with other tested Co/AC-
332 catalysts from the literature [40].

333

334 ***3.3 Surface functional groups***

335 Functional groups of activated carbon surface were determined by diffuse reflectance Fourier transformed
336 IR (DRIFT) analysis and it was possible to identify some of the oxygen-containing functionality. One of the
337 problems using infrared spectroscopy (FTIR) of carbonaceous materials is that they are effective black body
338 absorbers and are too opaque for direct transmission analysis on the mid-infrared spectral region. The
339 addition of KBr intensifies the signal but the signal is still too weak to obtain. An alternative technique is to
340 use (DRIFT) [41, 42]. Although IR spectroscopy does not provide quantitative information about carbon
341 surface chemistry, it can identify groups created or destroyed. Produced AC's were compared with
342 commercial AC. Main peaks at area 3400 cm^{-1}, 1620 cm^{-1} and 1620 cm^{-1} can be found from all AC's. From the
343 spectrum (Figure 6), few changes with different AC's peaks can be detected at the area 1000-2000 cm^{-1}.
344 Notable changes with peaks from AC treated with HNO_3 were at area 1760 cm^{-1} (carbonyl stretching of
345 quinones and carboxylic acids), 1590 cm^{-1} (C=C stretching in the form of aromatic rings) and 1240 cm^{-1} (C-O
346 stretches presumably from both carboxylic acid groups and phenolic hydroxyls) [43, 44]. Peaks at 1570 cm^{-1},
347 1380 cm^{-1} and 1240 cm^{-1} might also indicate to C=N structure[23].

348 XPS measurements were performed for calcined but not reduced Co/AC-catalysts to get more specific
349 information from functional groups on activated carbon, especially carbon-oxygen, and cobalt complexes.

350 Figure 7a shows the high resolution C1s-spectra and reveals components corresponding carbidic carbon (*BE*=
351 282.6-282.9 eV); graphitic or aliphatic carbon (*BE*= 284.6-285.1 eV); carbon species in alcohol or ether groups
352 (*BE*= 286.3-287.0 eV); carbon in carbonyl groups (*BE*= 287.5-288.1 eV); carbon in carboxyl or ester groups
353 (*BE*= 289.3-290.0 eV); and shake-up satellite due π-π* transition in aromatic rings (*BE*= 291.2-292.1 eV). Peaks

in the region 286.3-287.5 eV may also present of structures C-N [45, 46]. From Table 9 can be seen that most of the carbon atoms present in the catalyst are graphitic/aliphatic and about 15-20 % is in carbon-oxygen (or C-N) compounds.

XPS spectrum of O1s-scans is presented in Figure 7b. and represents the oxygen groups on the surface of the catalyst. In the O1s-spectra functional oxygen groups are divided in three different peaks representing double bonded oxygen (C=O) to carbon in carbonyl, carboxyl, oxygen of quinone groups (*BE*= 530.4-530.8 eV); single bonded oxygen (C-O) in alcohol or ester groups (*BE*= 532.4-533.1 eV) and chemisorbed oxygen or water (*BE*= 534.8-535.6 eV). Results showed that oxygen is in the form of double bonded oxygen and single bonded oxygen quite evenly (Table 9). Moreover, catalyst AC-Co-US contained more of double bonded oxygen (carbonyl/carboxyl) compounds than other catalysts while catalyst AC-HNO_3-Co-IW contained the least oxygen-containing groups from the catalysts.

XPS results of N1s-scans are presented in Table 9. The intensities of peaks from N1s spectrum was low but showed that catalysts AC-Co-PR and AC-HNO_3-Co-IW contained more nitrogen than other catalysts.

The Co2p-scan XPS results of the catalysts (Figure 7c) highlighted that, as already confirmed by the TPR, Co is present in its oxidized forms Co_3O_4, Co_2O_3 and CoO (BE= 779-782 eV) and no Co^0 (*BE*= 778 eV) has been found in any of the catalysts [47]. The lack of metallic Co is attributable to the fact that the Co-precursor used has an oxidation state equal to +3 and no further reduction treatments have been applied before XPS analysis.

Figure 8 highlights that the treatment with ultrasound causes a huge decrease in the content of graphitic or aliphatic carbon in AC-Co-US catalyst. It is wide discussed that ultrasounds are capable of degrading carbonyls and moreover a suitable technique to degrade graphite into other compounds [48, 49].

4. Conclusions

A series of Co-based catalysts supported on activated carbon and eventually promoted with Ru or Re have been synthesized and characterized. Different pretreatments and metal addition procedures seemed to have a high impact to the prepared Co-catalyst.

Prepared carbon support seemed to have many attractive properties including high specific surface area, proper pore distribution and high volume of mesopores and rather low ash value, which could be decreased even to zero by acid treatment. Acid treatment seemed to be important for removing inorganic compounds e.g. metals from the carbon support, which might affect to catalytic activity. Analyses including ICP-OES, SEM, TEM and XRD indicated that cobalt was successfully added onto carbon support in all catalyst preparation cases.

Some of the prepared Co-catalysts seemed to have good qualities (for FT-catalyst). Rather high dispersion (10.1 %) of the active metal (cobalt) was measured with Co-catalyst prepared by ultrasonic assisted impregnation method. Otherwise, there was an indication that a small metal particle size was difficult to reduce (TPO). TPR results highlighted that carbon supported cobalt catalysts proved to have lower reduction temperatures referred to the second reduction step of cobalt oxide to metallic cobalt if compared with SiO_2 supported FT catalyst. Moreover, pretreatment with HNO_3 seemed to have a positive effect on reduction temperatures and to a degree of reduction compared to other prepared Co/AC-catalysts. Also, the addition of the promoter Re did seem to improve the reduction degree of cobalt as measured in the TPO measurements. According to XPS analyses, different preparation techniques seemed to have an impact on the catalyst surface structure. Further, these prepared cobalt catalysts needs a thorough testing in the pilot scale FT plant.

5. Acknowledgements

The authors acknowledge the EU/European Regional Development Fund, Leverage from the EU program (within project nr. A71029) for financial support.

6. References

[1] Demirbaş A, Arslan G, Pehlivan E (2006) Energy Sources, Part A: Recovery, Utilization, and Environmental Effects 28:627-638

[2] Lam E, Luong JHT (2014) ACS Catalysis 4:3393-3410

[3] Rodríguez-Reinoso F (1998) Carbon 36:159-175.

[4] Bezemer GL, Radstake PB, Falke U, Oosterbeek H, Kuipers HPCE, van Dillen AJ, et al. (2006) Journal of Catalysis 237:152-161.

[5] Khodakov AY (2009) Catalysis Today 144:251-257

[6] Jean-Marie A, Griboval-Constant A, Khodakov AY, Diehl F (2009) Comptes Rendus Chimie 12:660-667

[7] Tsakoumis NE, Rønning M, Borg Ø, Rytter E, Holmen A (2010) Catalysis Today 154:162-182

[8] Iglesia E (1997) Applied Catalysis A: General 161:59-78

[9] Gnanamani MK, Jacobs G, Shafer WD, Davis BH (2013) Catalysis Today 215:13-17

[10] van Steen E, Prinsloo FF (2002) Catalysis Today 71:327-334

[11] Zaman M, Khodadi A, Mortazavi Y (2009) Fuel Processing Technology 90:1214-1219

[12] Serp P, Machado B (2015) Carbon (Nano) Materials for Catalysis, Nanostructured Carbon Materials for Catalysis, the Royal Society of Chemistry, pp. 1-45

[13] Fu T, Li Z (2015) Chemical Engineering Science 135:3-20

[14] Bitter JH, de Jong KP (2008) Preparation of Carbon-Supported Metal Catalysts, In: Serp P, Figueiredo JL (Eds) Carbon Materials for Catalysis. John Wiley & Sons, Inc., pp. 157-176

[15] Moreno-Castilla C, Ferro-Garcia MA, Joly J P, Bautista-Toledo I, Carrasco-Marin F, Rivera-Utrilla J (1995) Langmuir 11:4386-4392

[16] Kang J, Zhang S, Zhang Q, Wang Y (2009) TOC 121:2603-2606

[17] Kogelbauer A, Goodwin JG, Oukaci R (1996) Journal of Catalysis 160:125-133

[18] Eschemann TO, Oenema J, de Jong KP (2016) Catalysis Today 261:60-66

[19] Jacobs G, Das TK, Zhang Y, Li J, Racoillet G, Davis BH (2002) Applied Catalysis A: General 233:263-281

[20] Shu S, Guo J, Liu X, Wang X, Yin H, Luo D (2016) Applied Surface Science, Part B 360:684-692

[21] Zabihi M, Khorasheh F, Shayegan J (2015) Reaction Kinetics, Mechanisms and Catalysis 114:611-628

[22] Munnik P, de Jongh PE, de Jong KP (2015) Chemical Reviews 115:6687-6718

[23] Serp P, Joseph JL (2009) Carbon Materials for Catalysis, Wiley, Canada

[24] Khodakov AY, Chu W, Fongarland P (2007) Chemical Reviews 107:1692-1744

[25] Zowtiak JM, Bartholomew CH (1983) Journal of Catalysis 83:107-120

[26] Reuel RC, Bartholomew CH (1984) Journal of Catalysis 85:63-77

[27] Kababji AH, Joseph B, Wolan JT (2009) Catalysis Letters 130:72-78

[28] Maitlis MP, de Klerk A (2013) Greener Fischer-Tropsch Processes for Fuels and Feedstocks, Wiley-VCH

[29] Romar H, Lillebo AH, Tynjala P, Hu T, Holmen A, Blekkan EA, Lassi U (2016) Journal of Materials Science Research 5:39-49

[30] Tsakoumis NE, Rønning M, Borg Ø, Rytter E, Holmen (2010) A Catalysis Today 154:162–182

[31] Lillebø AH, Patanou E, Yang J, Blekkan EA, Holmen A (2013) Catalysis Today 215:60–66

[32] Song X, et al. (2013) Applied Catalysis A: General Volume 452:155–162

[33] Beswick O, et al. (2017) Catalysis Today 279, Part 1:29–35

[34] Wang T, Dinga Y, Xionga J, Yana L, Zhua H, Lua Y (2006) Catalysis Letters 107:47-52

[35] Comazzi A, Pirola C, Di Michele A, Compagnoni M, Galli F, Rossetti I, et al. (2016) Applied Catalysis A: General 520:92-98

[36] Lin H, Chen Y (2004) Materials Chemistry and Physics 85:171-175

[37] Olusola OJ, Sudip M (2016) Journal of Petroleum Technology and Alternative Fuels 7:1-12

[38] Ming H, Baker BG (1995) Applied Catalysis A: General 123:23-36

[39] Borg Ø, et al. (2007) Journal of Catalysis 248:89-100

[40] Zhang, Y, et al. (2007) Fischer-Tropsch synthesis, Catalysts and Catalysis, Edit, Davis BH and Occelli ML, p.87-99

[41] Jagiello J (1994) Langmuir 10:2778-2785

[42] Moreno-Castilla C, López-Ramón MV, Carrasco-Marín F (2000) Carbon 38:1995-2001

[43] Dandekar A, Baker R, Vannice M (1998) Carbon 36:1821-1831

[44] Mangun CL, Benak KR, Daley MA, Economy J (1999) Chemistry of Materials 11: 3476-3483

[45] Biniak S, Szymański G, Siedlewski J, Świtkowski A (1997) Carbon 35:1799-1810

[46] Nahil MA, Williams PT (2012) Waste Biomass Valor 3:117-130

[47] Biesinger MC, et.al (2011) Applied Surface Science 257:2717-2730

[48] Suslick KS, Hyeon T, Fang M, Cichowlas AA (1995) Materials Science and Engineering: A 204:186-192

[49] Guittoneau F, Abdelouas A, Grambow B, Huclier S (2010) Ultrasonics Sonochemistry 17:391-398

Lahti *et al*. Table captions

Table 1. A summary of catalyst denotation: precursor salts, impregnation methods and calcination.

Lahti et al. Tab 1.

Catalyst	Metal content	Metal salts used	Impregnation method used	Calcination
AC-Co-IW	10 wt. % Co	$Co(NO_3)_2{\cdot}6H_2O$	incipient wetness	320°C, 16h, N_2-flow
AC-HCl-Co-IW*	10 wt. % Co	$Co(NO_3)_2{\cdot}6H_2O$	incipient wetness	320°C, 16h, N_2-flow
AC-HNO_3-Co-IW**	10 wt. % Co	$Co(NO_3)_2{\cdot}6H_2O$	incipient wetness	320°C, 16h, N_2-flow
AC-CoRu-IW	10 wt. % Co 0.2 wt. % Ru	$Co(NO_3)_2{\cdot}6H_2O$ $Ru(NO)(NO_3)_3$	one-step incipient wetness	320°C, 16h, N_2-flow
AC-CoRe-IW	10wt. % Co 0.2 wt. % Re	$Co(NO_3)_2{\cdot}6H_2O$ ReO_4H	one-step incipient wetness	320°C, 16h, N_2-flow
AC-Co-PR	10 wt. % Co	$Co(NO_3)_2{\cdot}6H_2O$	precipitation with urea	320°C, 16h, N_2-flow
AC-Co-US	10 wt. % Co	$Co(NO_3)_2{\cdot}6H_2O$	ultrasonic assisted incipient wetness	320°C, 16h, N_2-flow

*) AC demineralized with HCl and **) AC oxidized with HNO_3 before impregnation.

Lahti *et al*. Table captions

Table 2. Surface area, pore volume, pore size, pore distribution, total carbon content and ash content of the raw lignin, activated carbon and acid treated activated carbons.

539 Lahti et al. Tab 2.

540

Sample	BET			BJH pore distribution				
	Surface area (m^2/g)	Pore volume (cm^3/g)	Pore size (nm)	Micro-pores (%)	Meso-pores (%)	Macro-pores (%)	Carbon content (%)	Ash (%)
Lignin, untreated	4.6	0.02	18	n.d.	n.d.	n.d.	65	n.d.
AC	810	0.41	2	32	62	6	96	6.1
AC, treated with HCl	822	0.41	2	34	60	6	95	4.8
AC, treated with HNO_3	714	0.35	2	33	61	6	85	0.0

541 n.d. = not determined

542

543

544

545

546

547

548

549

550

551

552

553

Lahti *et al*. Table captions

Table 3. Elemental analysis (C, H, O, N) for activated carbon supports.

574 Lahti et al. Tab 3.

575

Sample	Treatment	C (%)	H (%)	O (%)	N (%)
AC	Untreated	86.4	0.7	2.2	0.6
AC	30% HNO_3, reflux 3h	59.6	1.9	0	1.4
AC	30% HCl, reflux 3h	79.8	1.2	4.3	0.5

576

577

578

579

580

581

582

583

584

585

586

587

588

589

Lahti *et al*. Table captions

Table 4. Surface area, pore volume, pore size, cobalt metal dispersion, metal particle size and metal surface area of Co/AC-catalysts.

611 Lahti et al. Tab 4.

612

613

Catalyst*	BET Surface area (m^2/g)	Pore volume (cm^3/g)	Average pore size (nm)	Co metal dispersion (%)	Co metal particle size (nm)	Co metal surface area (m^2/g sample)	Co metal surface area (m^2/g of metal)
AC-Co-IW	710	0.35	2	8.6	11.6	5.8	58.1
AC- HCl-Co-IW	610	0.30	2	0.7	138.5	0.5	4.9
AC-HNO_3-Co-IW	640	0.32	2	3.4	29.8	2.3	22.7
AC-CoRu-IW	640	0.29	2	3.2	31.0	2.2	21.8
AC-CoRe-IW	630	0.31	2	5.8	17.2	3.9	39.2
AC-Co-PR	680	0.34	2	n.d.	n.d.	n.d.	n.d.
AC-Co-US	600	0.28	2	10.1	9.8	6.9	68.6

614 *) Preparation methods presented in Table 1.
615 n.d. = not determined
616
617

618

619

620

621

622

623

624

625

626

Lahti *et al*. Table captions

Table 5. Metal content in catalysts from ICP analysis.

Lahti et al. Table 5.

Catalyst	Co wt.%	Ru wt.%	Re wt.%	Ca wt.%	Fe wt.%	Na wt.%	K wt.%	Mg wt.%
AC-Co-IW	5.9			0.02	0.02	0.30	0.11	<0.01
AC-HCl-Co-IW	11.1			0.02	0.01	0.01	<0.01	<0.01
AC-HNO_3-Co-IW	8.3			0.02	0.01	0.01	<0.01	<0.01
AC-CoRe-IW	9.1		0.39	0.03	0.03	0.35	0.10	0.02
AC-CoRu-IW	9.3	0.24		0.04	0.06	0.13	0.07	0.03
AC-Co-PR	9.2			0.01	0.02	0.25	0.09	<0.01
AC-Co-US	9.8			0.04	0.06	0.21	0.07	0.03

Lahti *et al*. Table captions

Table 6. SEM-EDS spectrum labels from catalyst AC-HNO_3-Co-IW.

Lahti et al. Tab 6.

Spectrum Label	S147	S148	S149	S150	S151	S152	S153	S154	S155	S156
C	26.22	20.98	35.43	20.39	27.05	63.41	22.03	24.76	35.54	22.52
O	1.06	20.11	2.40	0.71	1.40	8.44	0.85	0.99	15.91	0.84
Co	71.82	58.53	60.49	75.82	70.36	27.39	76.10	72.67	48.19	75.32

Lahti *et al*. Table captions

Table 7. Temperatures (°C) for reduction steps and total H_2-consumption.

729 Lahti et al. Tab 7.

730

Catalyst	Phase transformation T (°C)		Total H_2-consumption ($mmol/g_{cat}$)
	$Co_3O_4 \rightarrow CoO$	$CoO \rightarrow Co^0$	
AC-Co-IW	330	480	4.0
AC-HCl-Co-IW	350	410	3.3
AC-HNO_3-Co-IW	320	370	6.3
AC-CoRu-IW	330	420	7.0
AC-CoRe-IW	380	480	5.2
AC-Co-PR	340	470	5.0
AC-Co-US	340	490	5.7
Co-SiO_2	260	780	n.d.

731

732

733

734

735

736

737

738

739

740

741

Lahti *et al*. Table captions

Table 8. The degree of reduction at 350°C and volume of O_2 adsorbed on the catalyst surface.

762 Lahti et al. Tab 8.

763

Catalyst	O_2-consumption (ml/g_{cat})	Degree of reduction (%)
AC-Co-IW	1.2	39
AC-HCl-Co-IW	2.2	37
AC-HNO_3-Co-IW	1.9	66
AC-CoRu-IW	1.9	38
AC-CoRe-IW	2.2	72
AC-Co-PR	1.8	45
AC-Co-US	1.3	25

764

765

766

767

768

769

770

771

772

773

774

775

776

Lahti *et al*. Table captions

Table 9. Spectral parameters of C1s-, O1s-, Co2p- and N1s-scans of catalysts.

801 Lahti et al. Tab 9.

802

Scan	Binding Energy (eV)	AC-Co-IW (A%)	AC-HCl-Co-IW (A%)	AC-HNO_3-Co-IW (A%)	AC-CoRu-IW (A%)	AC-CoRe-IW (A%)	AC-Co-PR (A%)	AC-Co-US (A%)
C1s Scan								
carbidic carbon	282				7.0			
graphitic or aliphatic carbon	284–285	47.6	47.8	50.7	36.2	28.8	46.8	19.8
carbon in ethers, alcohols, phenols, amines, carbonyls, quinones, carboxyl or ester groups	286–291	12.6	13.0	21.9	14.7	9.8	11.8	7.9
π-π* shake-up peaks	291–292	12.7	12.5	9.3	14.0	7.9	11.2	10.0
O1s Scan								
C=O groups	530	9.1	10.6	9.5	11.3	25.3	12.0	32.8
C-OH, C-O-C groups	532–533	10.0	8.4	2.9	9.0	14.7	9.1	11.0
chemisorbed O or water	534–536	3.6	2.4	0.9	3.5	4.2	2.9	5.9
Co2p Scan	779–782	4.0	4.8	0.9	4.6	6.0	4.8	13.8
N1s Scan	399	0.4	0.4	1.0	0.5	0.5	1.9	0.3

803 The peak area is calculated for each sample as atomic percent ratio

804

805

806

Lahti *et al*. Figure captions

Figure 1. Scheme for the preparation methods of cobalt catalysts on activated carbon support.

827 Lahti et al. Fig 1.

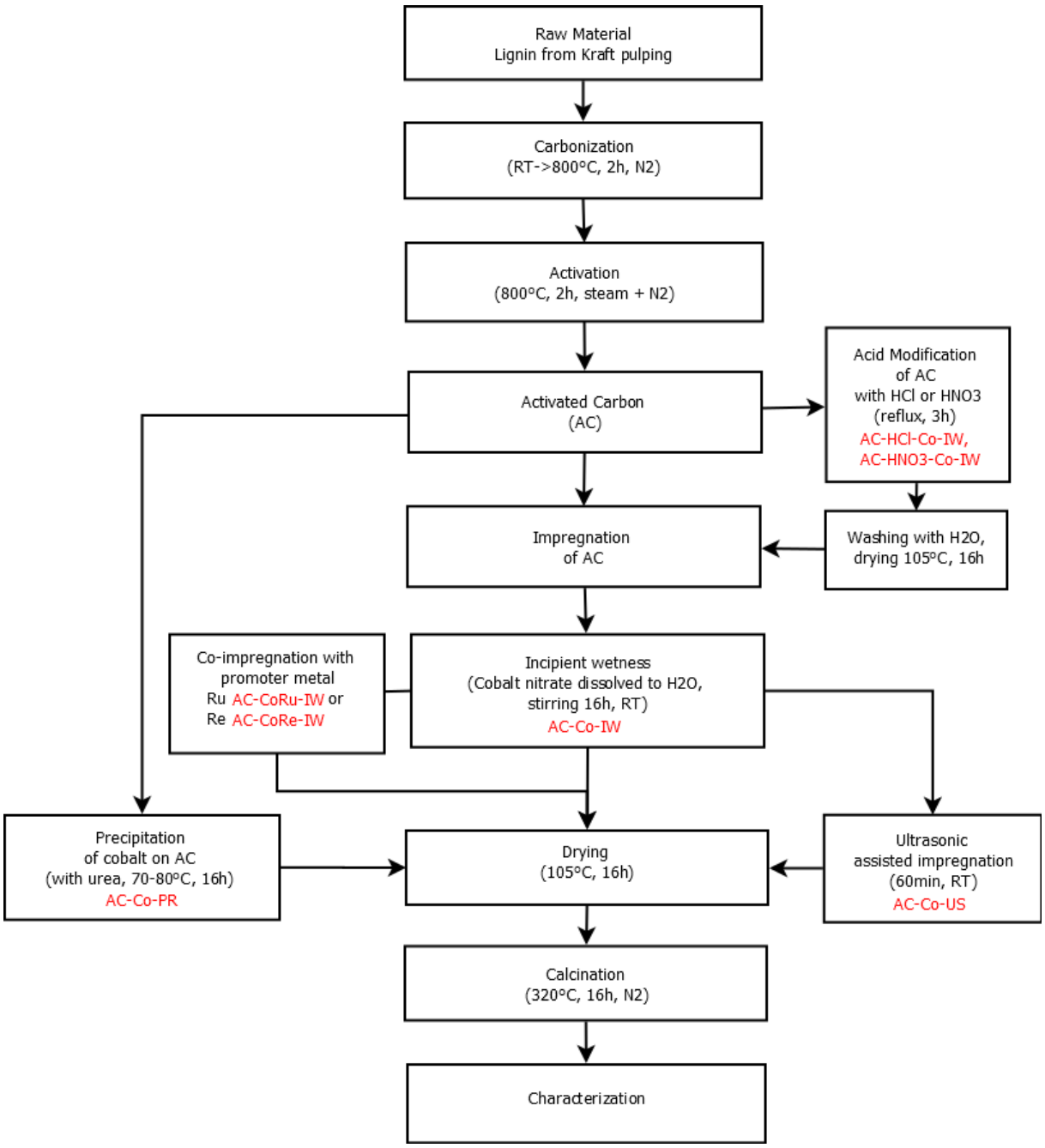

828

829

830

831

Lahti *et al*. Figure captions

Figure 2. FESEM (left) and TEM (right) images of catalyst AC-Co-IW.

852 Lahti et al. Fig 2.

853

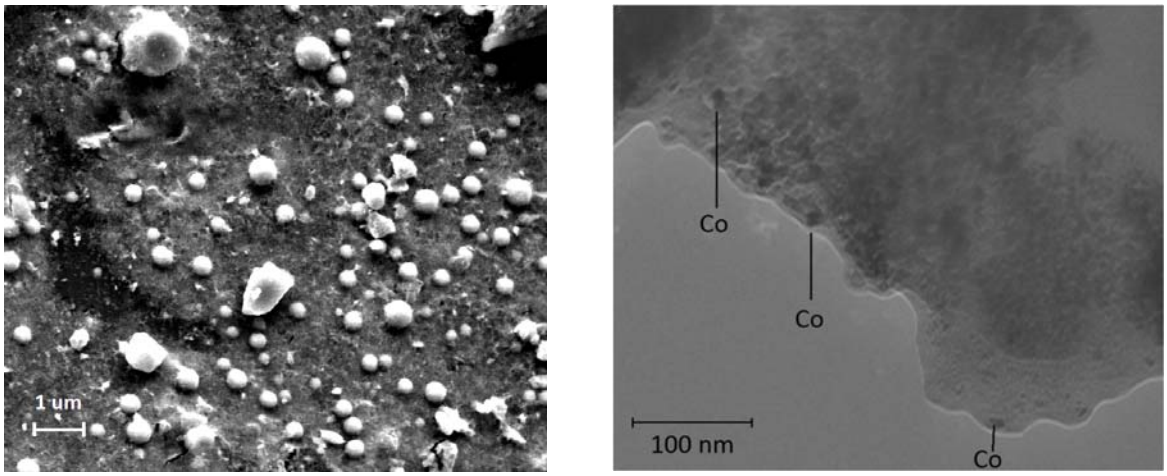

854

855

856

857

858

859

860

861

862

863

864

865

Lahti *et al*. Figure captions

Figure 3. SEM-EDS spectrum from catalyst AC-HNO_3-Co-IW.

886 Lahti et al. Fig 3.

887

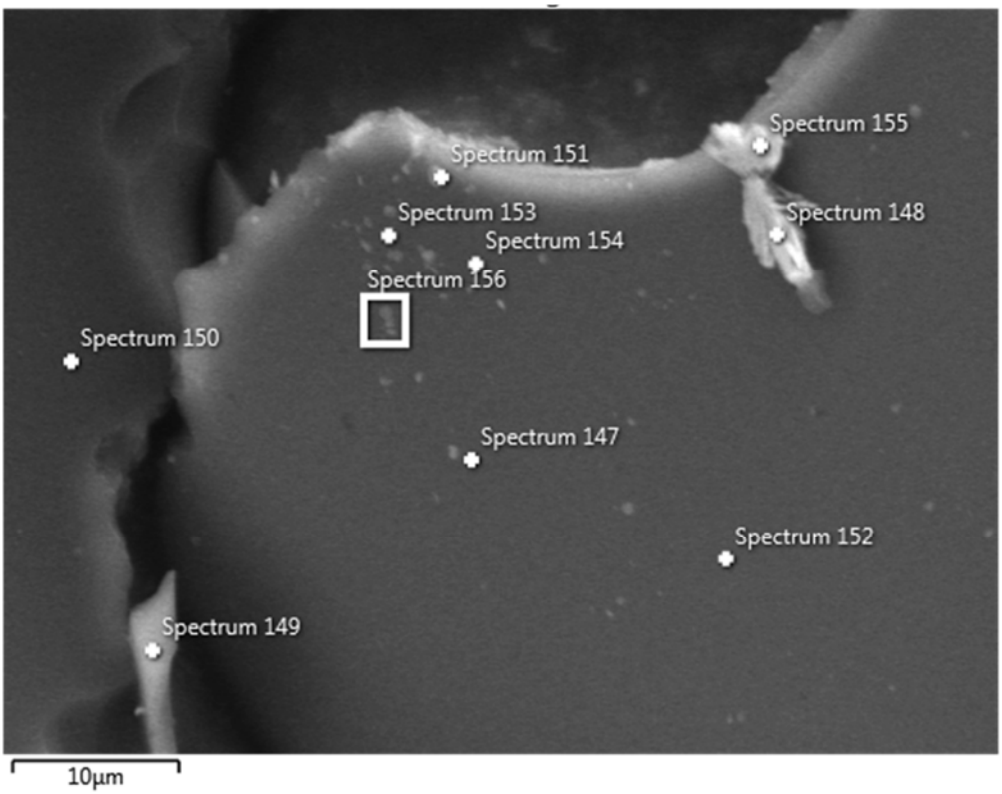

888

889

890

891

892

893

894

895

896

897

Lahti *et al*. Figure captions

Figure 4. XRD diffraction pattern of Co/AC-catalysts.

Lahti et al. Fig 4.

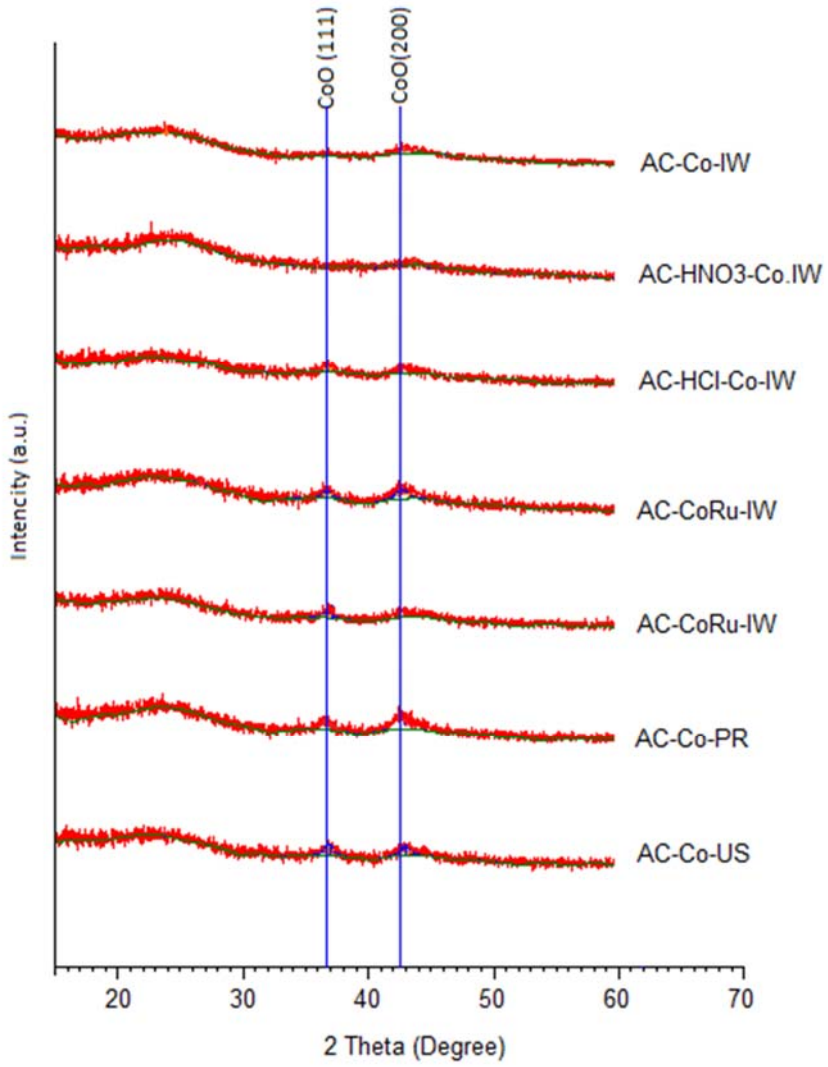

Lahti *et al*. Figure captions

Figure 5. H_2-TPR profiles for AC supported and SiO_2 supported Co-catalysts.

946 Lahti et al. Fig 5.

947

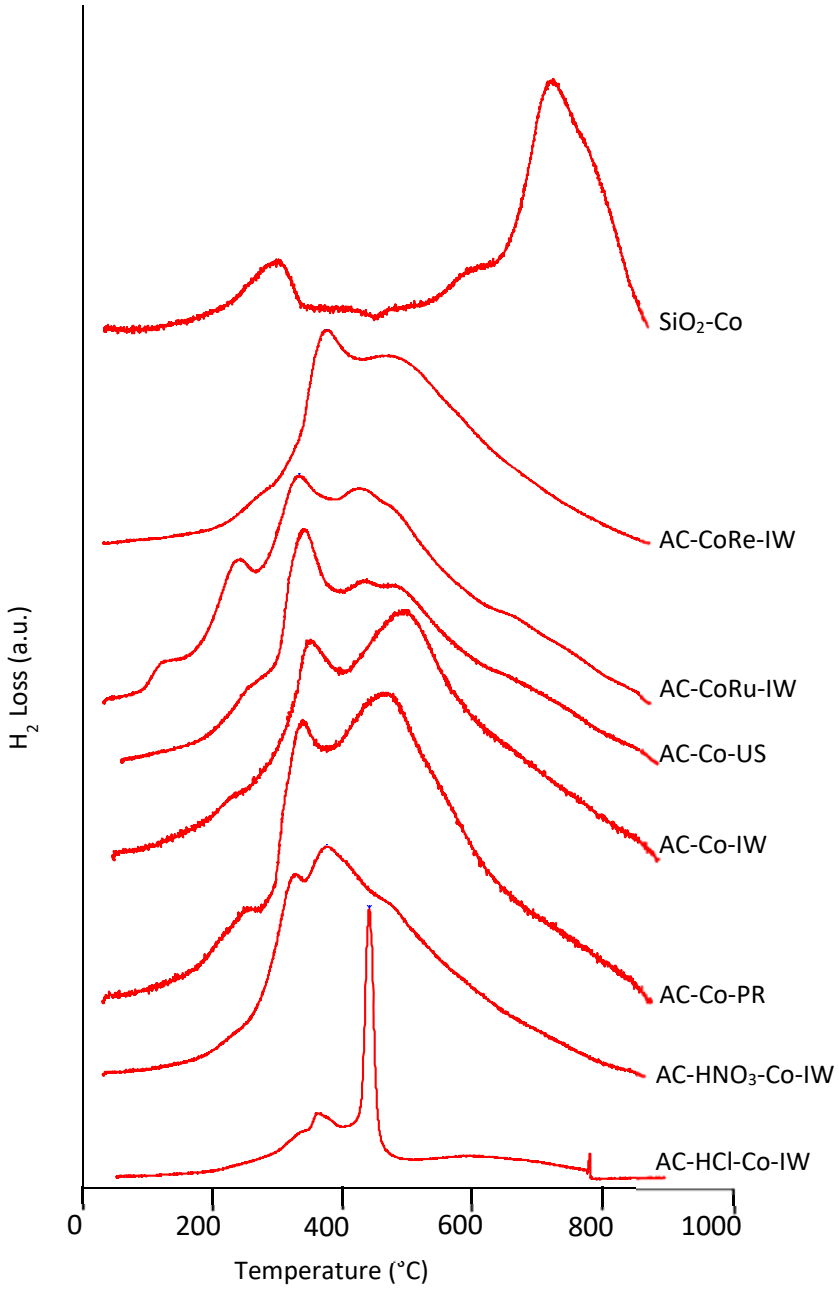

948

949

950

951 **Lahti *et al*. Figure captions**

952 Figure 6. DRIFTs spectrum for commercial AC, prepared AC and AC treated with HNO_3.

953

954

955

956

957

958

959

960

961

962

963

964

965

966

967

968

969

970

971 Lahti et al. Fig 6.

972

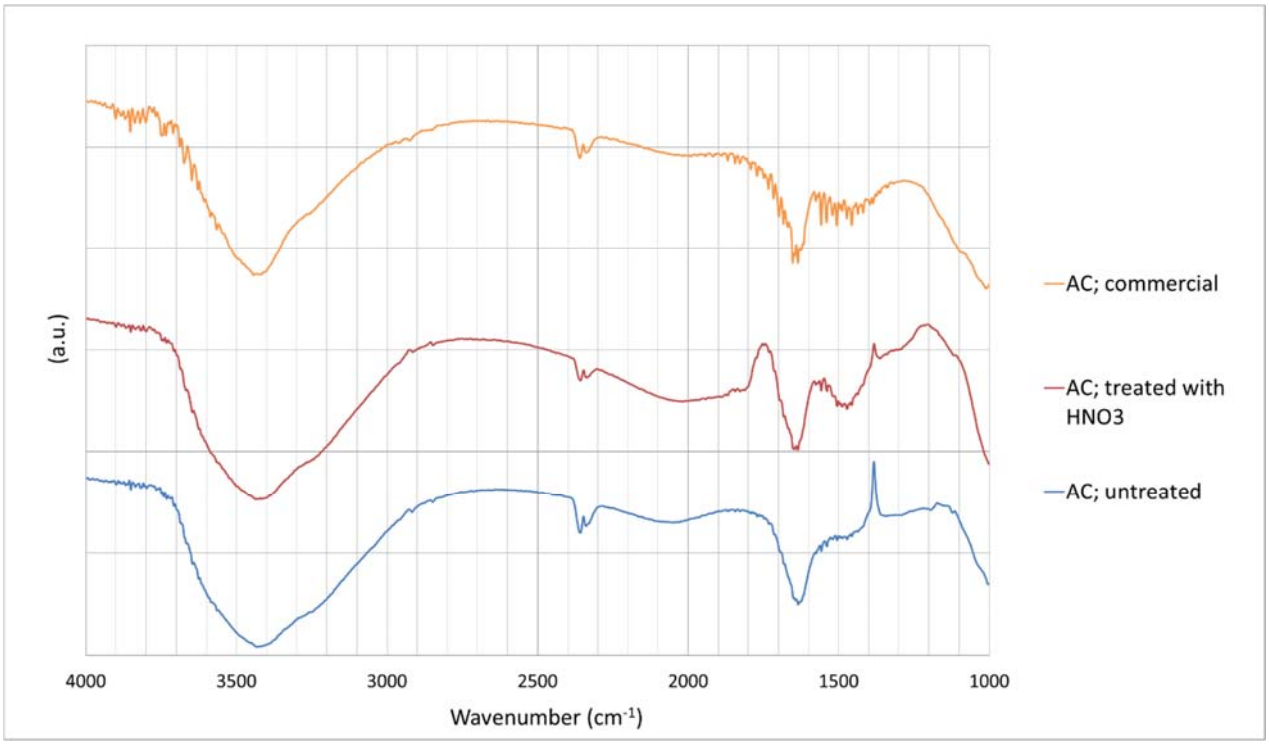

973

974

975

976

977

978

979

980

981

982

Lahti *et al*. Figure captions

Figure 7. High-resolution XPS spectrum of (a) C1s scans, (b) O1s scans, (c) Co2p -scans from Co/AC-catalysts.

1003 Lahti et al. Fig 7.

1004

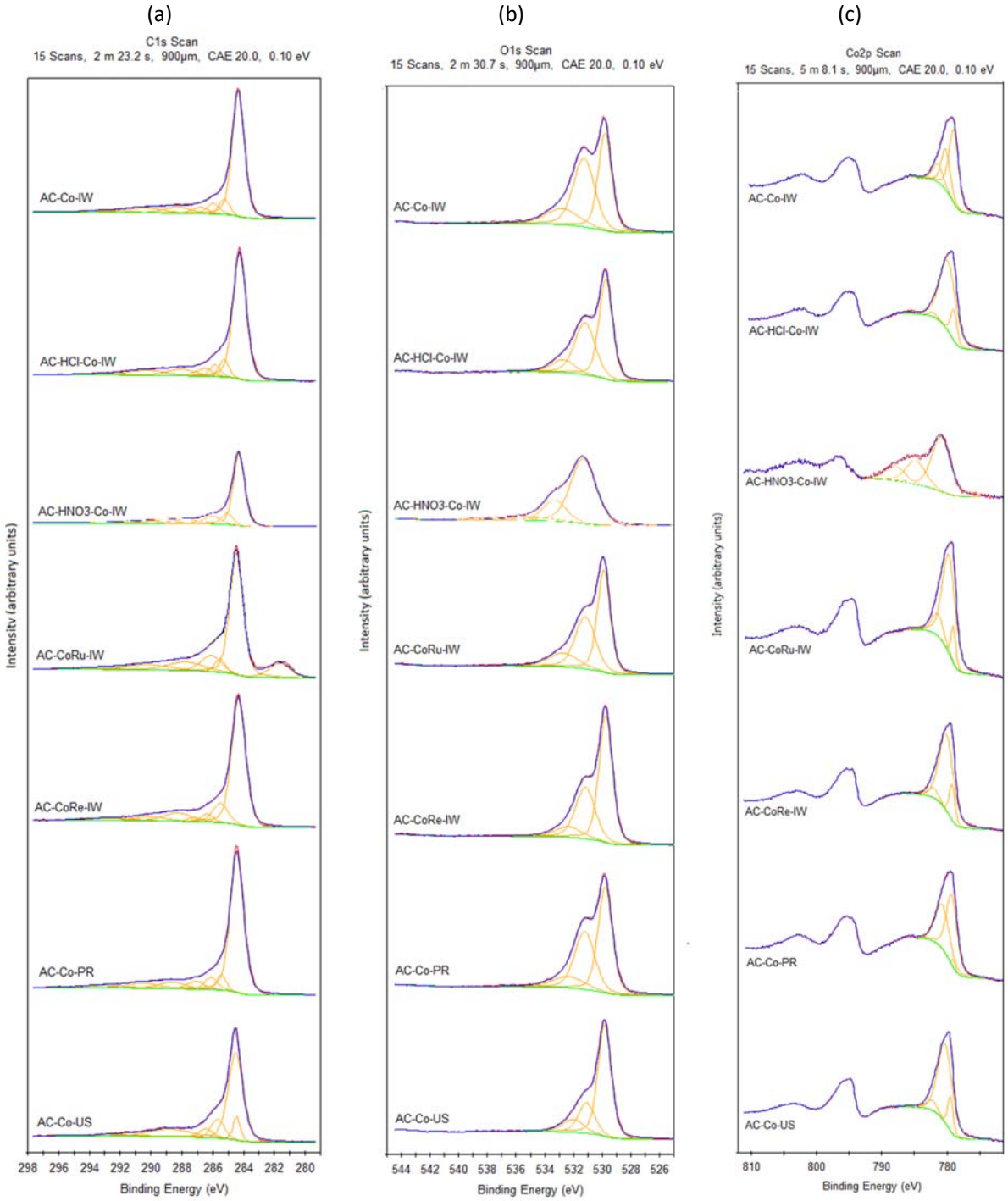

1005

1006

Lahti *et al*. Figure captions

Figure 8. Functional groups on carbon surface from C1s, O1s, and Co2p -scans.

1038 Lahti et al. Fig 8.

1039

1040

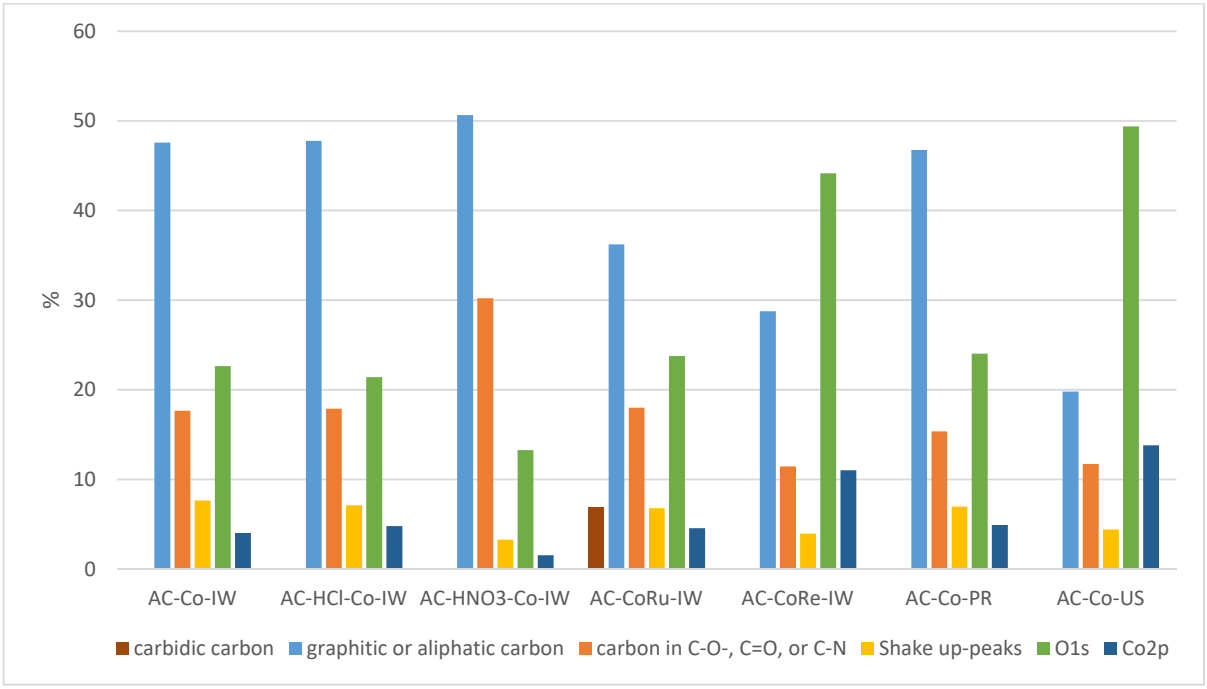

1041

1042

1043

1044

1045

1046

1047

1048

1049

1050

Referees

Professor Edd Anders Blekkan, edd.a.blekkan@ntnu.no

Professor Harry Bitter, j.h.bitter@uu.nl

Kari Cook, kari@cookengineer.com